Solar Physics (2005) 229: 213–226

ELECTRON ACCELERATION IN THE CORONA

G. M. SIMNETT
School of Physics and Astronomy, University of Birmingham, B15 2TT, UK (e-mail: gms@star.sr.bham.ac.uk)

(Received 26 January 2005; accepted 7 April 2005)

Abstract. The series of nine impulsive, highly collimated beams of near-relativistic electrons seen by ACE/EPAM on 26 and 27 June 2004 occurred at a quiet time with respect to solar flare and CME production. However, they were accompanied by decametric type III radio bursts observed by WIND/WAVES, which had progressively higher starting frequencies, suggestive of coronal acceleration. There were no CMEs seen by SOHO/LASCO in association with any of the type III bursts except possibly the first. The energy spectrum of the electrons was soft, typically $E^{-4.5}$ but extended up to at least ∼200 keV. We suggest that the source region for these events is in the high corona. We discuss this result in the context of solar electron acceleration at other times.

1. Introduction

The Sun is the engine responsible for populating the inner heliosphere with energetic particles, apart from those which are galactic cosmic rays, and those which are emitted from planetary magnetospheres. Yet the precise way this happens is still unclear. There has been much prominence given recently to the role of corona mass ejection (CME) driven shocks as the main source (Reames, 1999; Simnett, Roelof, and Haggerty, 2002) but the Sun produces a variety of transients which could accelerate charged particles, and it is difficult to know for certain which process is having which effect.

We concentrate here on the near-relativistic (38–315 keV) electrons detected by the EPAM instrument on the ACE spacecraft (see below). There are two important possible sources for such electron acceleration driven by solar transient activity outside of major flares. (1) Magnetic reconnection in the high corona (probably important for ions below around 1 MeV/nucleon and electrons below about 50 keV); (2) Acceleration at a CME-driven shock. The events we are discussing were not accompanied by major flares or significant coronal mass ejections. Thus, in the absence of both a flare and a CME, it is probable that (1) is the dominant mechanism. The events we discuss in this paper are believed to satisfy this condition, except possibly where noted.

In this paper we discuss only near-relativistic electron events, where the propagation from the Sun to the observing spacecraft at ∼1 AU is just tens of minutes, provided we restrict ourselves to energies significantly above the *strahl*, say above 30 keV. Here the velocity is around 1/3c, so the difference in transit time across 1 AU between a 30 keV electron and, say, a 10 MeV electron is only around 15 min.

Therefore we stand a much better chance of separating the effects of various possible sources if we restrict our observations to electrons above ∼30 keV.

The motivation for this study may be stated in the following way. Many observations of solar electrons show that the differential energy spectrum is often well-represented by a power law. However, the power law spectral index may have values ranging from ∼−1 to steeper than −6. Lin (1985) has shown that the observed electron spectrum at 1 AU from some events may be represented by more than one power law index, depending on the energy. One possibility to account for this is that the observations cover more than one discrete source, and that different sources typically have a different spectral index.

Suppose each of the various solar electron acceleration processes typically accelerates electrons with a characteristic spectral index at a time which may be deduced approximately from other data; for example, radio bursts, CME observations, X-ray data, etc. Then if the constraints provided by these data are known and understood the contribution of each source to a given observation may be identified. For example, if we know that the electrons from coronal acceleration typically have a very soft spectrum, then the detection of electrons with a very hard spectrum would then indicate a different source, e.g., a flare. The ultimate objective is to be able to establish the energetic particle output from flares so that the physics of the enigmatic solar flare may be revealed.

Some decades ago (Potter, Lin, and Anderson, 1980) it was established that some electron events seen at 1 AU probably originated in the high corona. At that time the unambiguous events they reported had low intensities and steep spectra, probably with a high energy cut-off below 30 keV. In this paper we identify what are probably coronal events but with much higher intensities and extending an order of magnitude higher in energy. If this hypothesis is correct, then it has important consequences for the study of energy release processes and particle acceleration in the corona, which may in turn aid our understanding of acceleration in flares and CMEs, as the coronal population may provide a seed population for further acceleration.

2. Observations

The observations we discuss are charged particle data from ACE/EPAM (Gold *et al.*, 1998); the decametric radio data from WIND/WAVES (Bougeret *et al.*, 1995); SOHO/LASCO coronagraph data (Brueckner *et al.*, 1995) and various ground-based data reported in *Solar Geophysical Data* (US Department of Commerce, Boulder, CO).

2.1. Charged particles

The events of interest occurred over a 24-h period from 20 UT 26 June, to 20 UT 27 June, 2004. We shall hereinafter omit the year. EPAM has four

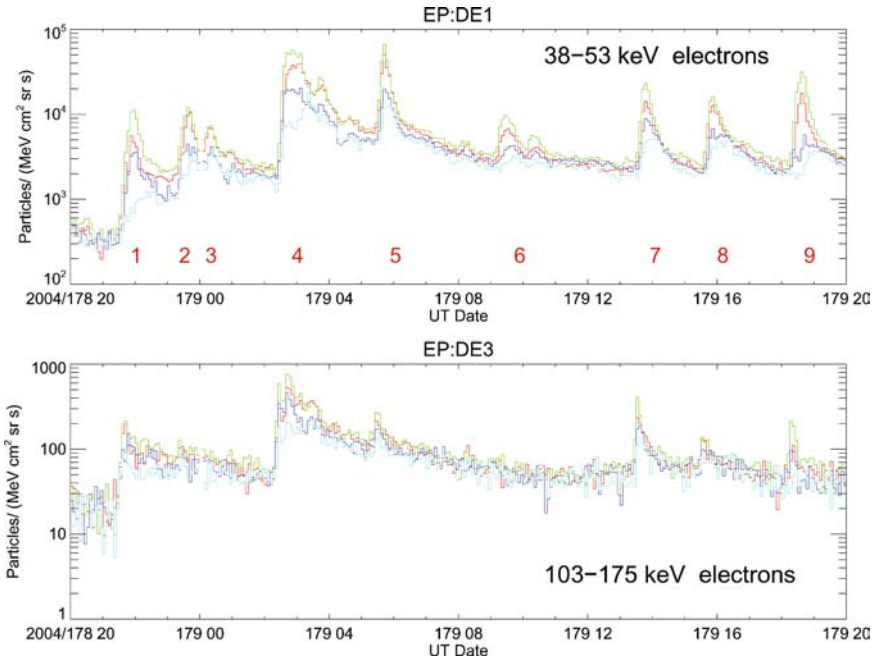

Figure 1. The 38–53 keV and 103–175 keV electron intensity for 26:20–27:20 June 2004 (DOY 178, 179). All four sectors are plotted as 5 min averages.

magnetically-deflected electron channels with energies 38–53–103–175–315 keV, which we refer to as DE1-4. The ACE spacecraft spins every 12 s, and the spin is divided into four equal 90° sectors. Figure 1 shows the 38–53 keV electron channel (DE1) and the 103–175 keV electron channel (DE3), with all four sectors plotted as 5 min averages. Nine events are indicated in the upper panel of Figure 1 and the number we have assigned to each event is given in the lower part of this panel. There are a further two events visible in the DE1 channel after events 4 and 6. We have not included these in our analysis as they did not have resolved peaks in the DE2 channel, and therefore we could not identify a spectrum for them. The centre of the aperture opening is at 30° to the spacecraft spin axis.

EPAM is a suite of 5 detectors, three of which respond to electrons. In addition to the magnetically-deflected electrons discussed above, there are two solid-state detector telescopes which have a thin foil in front to absorb low energy ions. These are the LEFS60 and LEFS150 detectors, which are mounted with the centres of the field-of-view at 60° and 150°, respectively to the spacecraft spin axis. The electron channels from LEFS60 are referred to as E′1-4 (accumulated over eight 45 degree sectors) and those from LEFS150 are E1-4. The full opening angle of all the EPAM telescopes is ∼50°. For most orientations of the interplanetary magnetic field with respect to the spacecraft spin axis, the three electron channels provide almost complete pitch angle coverage, as will be seen below (Figure 8).

The lower panel of Figure 1 is the 103–175 keV intensity, which does not show as many events as in DE1. However, there is velocity dispersion in these events, which is clearest in event 7, where DE3 starts to fall before DE1 has experienced much of an increase. The peak sector (Sector 2) is the peak sector in all events; however, as the electrons are propagating virtually scatter-free from the Sun, this merely reflects the relative quietness of the interplanetary medium with respect to magnetic field fluctuations. The sector number is simply used as a convenient reference, based on the spacecraft spin vector, and has no other significance.

To put this period into context we have examined the electron and ion intensities for one solar rotation, from 11 June to 8 July. The sector-averaged electron intensity is shown in Figure 2 for the four deflected electron channels. This solar rotation is relatively quiet, and the 24-h period shown in Figure 1 represents the only time the DE1 intensity was above 2×10^3 electrons/(MeV cm^2 sr s). Thus the interplanetary medium is not heavily populated with electrons from earlier solar events.

Figure 3 shows some representative ion channels from EPAM which are all from the LEMS120 detector (77–127 keV (P′2), 207–336 keV (P′4), 601–1123 keV (P′6) and 1874–4750 keV (P′8)). Not only are there no ion events correlating with the electron events in Figure 1, but the ion intensity in general is uncorrelated with the electrons, with very little activity above 1 MeV for the whole rotation. For

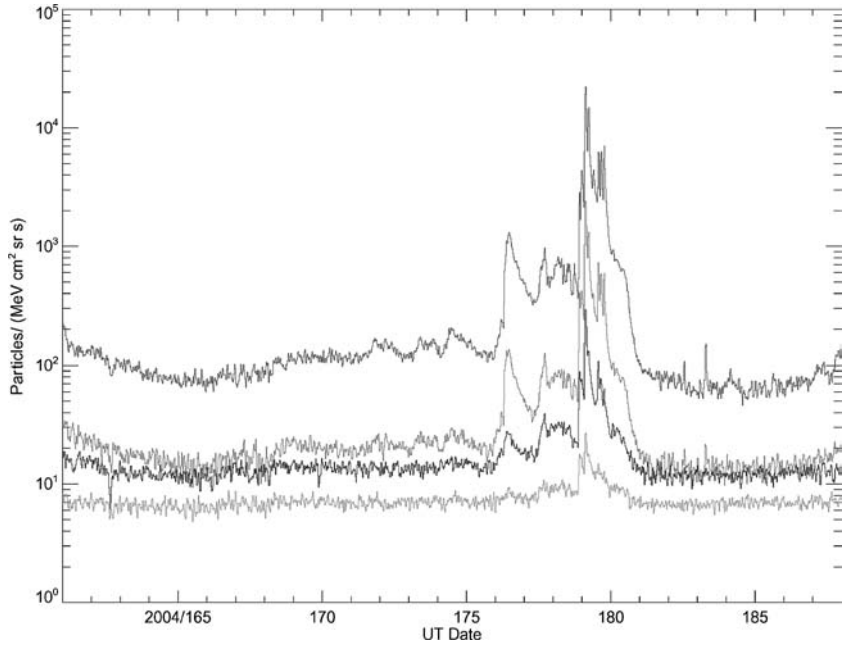

Figure 2. The electron intensity for a solar rotation from 11 June to 8 July, 2004. The data are plotted as hourly and spin averages. From the top the energy channels are: 38–53 keV (DE1); 53–103 keV (DE2); 103–175 keV (DE3); 175–315 keV(DE4).

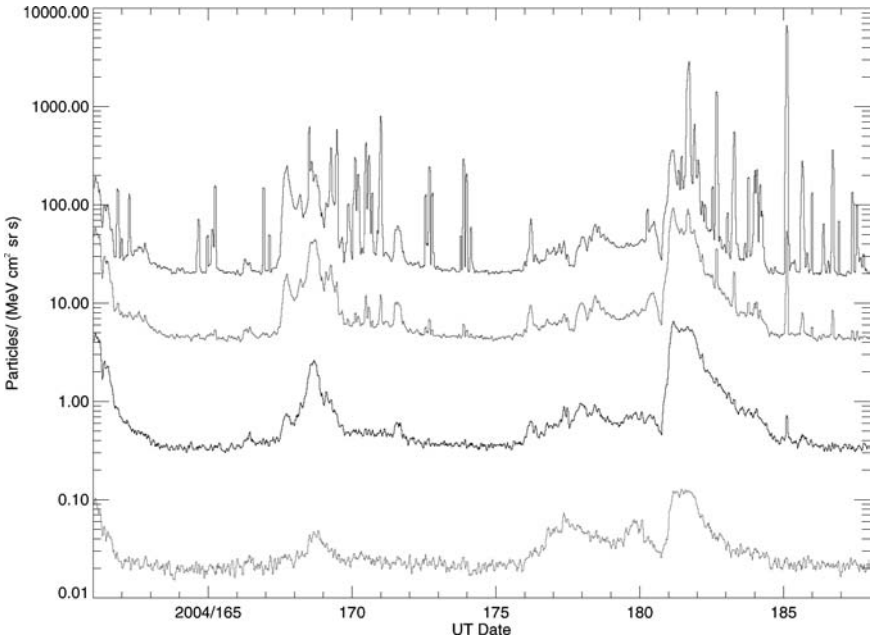

Figure 3. The ion intensity for a solar rotation from 11 June to 8 July, 2004. The data are plotted as hourly and spin averages. From the top the energy channels are: 77–127 keV (P′2); 207–336 keV (P′4); 601–1123 keV (P′6); 1874–4750 keV (P′8).

example, the 6–7 day period when the 77–127 keV ion intensity is never above 100 particles/(MeV cm^2 sr s) neatly encompasses the period when the DE1 electron intensity (Figure 2) is above 2×10^3/(MeV cm^2 sr s)!

The magnetic field at ACE, which is shown in Figure 4 for the three-day period 25–27 June, is declining during the 24 h of interest here from a small increase seen on the previous day. The data are plotted in RTN coordinates. This period is highlighted in Figure 4. The lack of short-term fluctuations for much of this interval is suggestive of a magnetic cloud; however, there are not strong rotational signatures in θ or ϕ, which are relatively constant within $\pm 30^\circ$ for the period of interest. Note that the radial component of the magnetic field is negative, which means the (conventional) direction is towards the Sun. (This is relevant to the pitch-angle distributions shown in Figure 7 below.)

We next turn to the electron spectrum. The differential energy spectrum may be represented by $\mathrm{d}J/\mathrm{d}E \propto E^{-\gamma}$ and the spectral index γ for the nine events is in the range 3.77–5.44. Figure 5 shows the spectrum at the maximum intensity in events 4 and 9. The spectra are derived from the peak intensity in each energy channel, and are thus not the instantaneous measured spectra. Figure 6 shows a histogram of the spectral index of the peak sector for all nine events. We note a slight trend towards a gradually steepening spectrum with time.

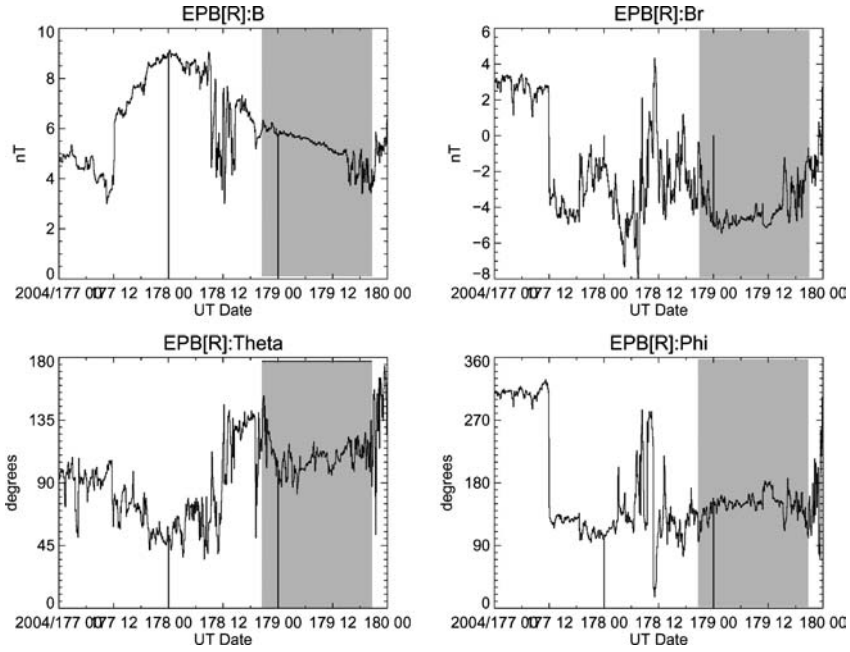

Figure 4. The magnetic field at ACE, in RTN coordinates, for the period 25–27 June, 2004 (DOY 177–179). The period of interest covering the electron events is shaded.

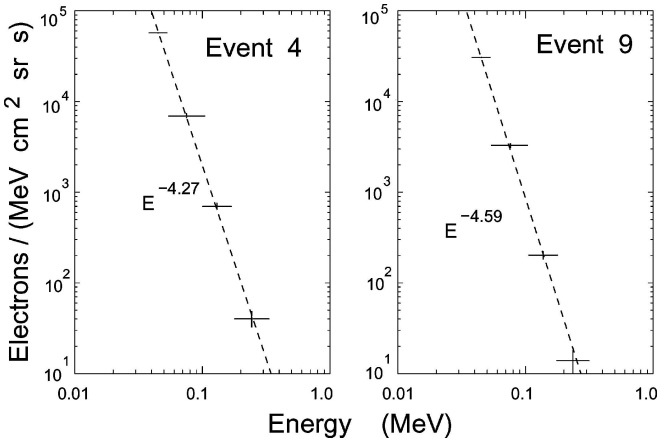

Figure 5. Left panel: The electron differential energy spectrum for event 4. *Right panel*: The same for event 9.

It is clear from the data in Figure 1 that the events are highly anisotropic. We now put this on a more quantitative basis by showing in Figure 7 the electron pitch-angle distribution for each event. For most events almost complete pitch angle coverage is provided by E2 and E′2, but for events 3, 5 and 7 some additional coverage is

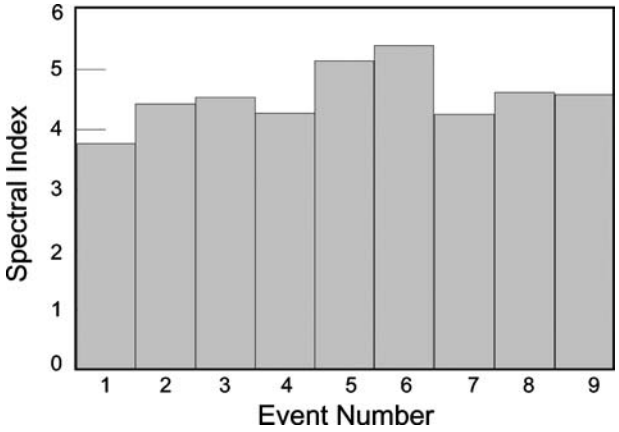

Figure 6. The electron differential energy spectral index for the nine events.

provided by DE2. Figure 4 indicates that the radial component of the interplanetary magnetic field is negative, which means that a field-aligned electron beam coming from the Sun will have a peak at a pitch cosine of -1. Typically for a short event with rapidly varying intensity the pitch-angle distribution from the two different detectors on EPAM will not necessarily reproduce exactly, which explains why the distributions for some events have a finite "width".

2.2. TYPE III RADIO BURSTS

When beams of electrons pass through the corona it is common for them to excite radiation at the local plasma frequency. The dynamic radio spectrum of the events then drifts rapidly to lower frequencies as the exciting beam moves to progressively lower coronal density. The WAVES instrument on the WIND spacecraft (Bougeret *et al.*, 1995) can monitor the passage of electron beams out to around 1 AU by observing at frequencies from around 14 to 1.075 MHz (RAD 2) and 1000 to 20 kHz (RAD 1). At typical coronal electron densities RAD 2 covers altitudes from around 2 to $6R_{\odot}$, while RAD 1 covers the remaining distance to around 1 AU. The frequency – density relationship is discussed in detail by Leblanc, Dulk, and Bougeret (1998). It should be noted that their discussion supposes that the corona is spherically-symmetric. It is always possible that locally the coronal density might depart from this model, due to, say a streamer. If this were to be the case, then the derived heights would be invalid. However, it is more probable that an inhomogeneity would be in the nature of a density enhancement rather than a depletion, which would lead to an underestimate of the altitude.

Figure 8 shows the dynamic spectrum from the WAVES/RAD2/ RAD1 receivers from 26 June 20:00 UT to 27 June 20:00 UT, 2004. The break between RAD2 and RAD1 is visible as a slight discontinuity in intensity around 1000 kHz. On 26 June

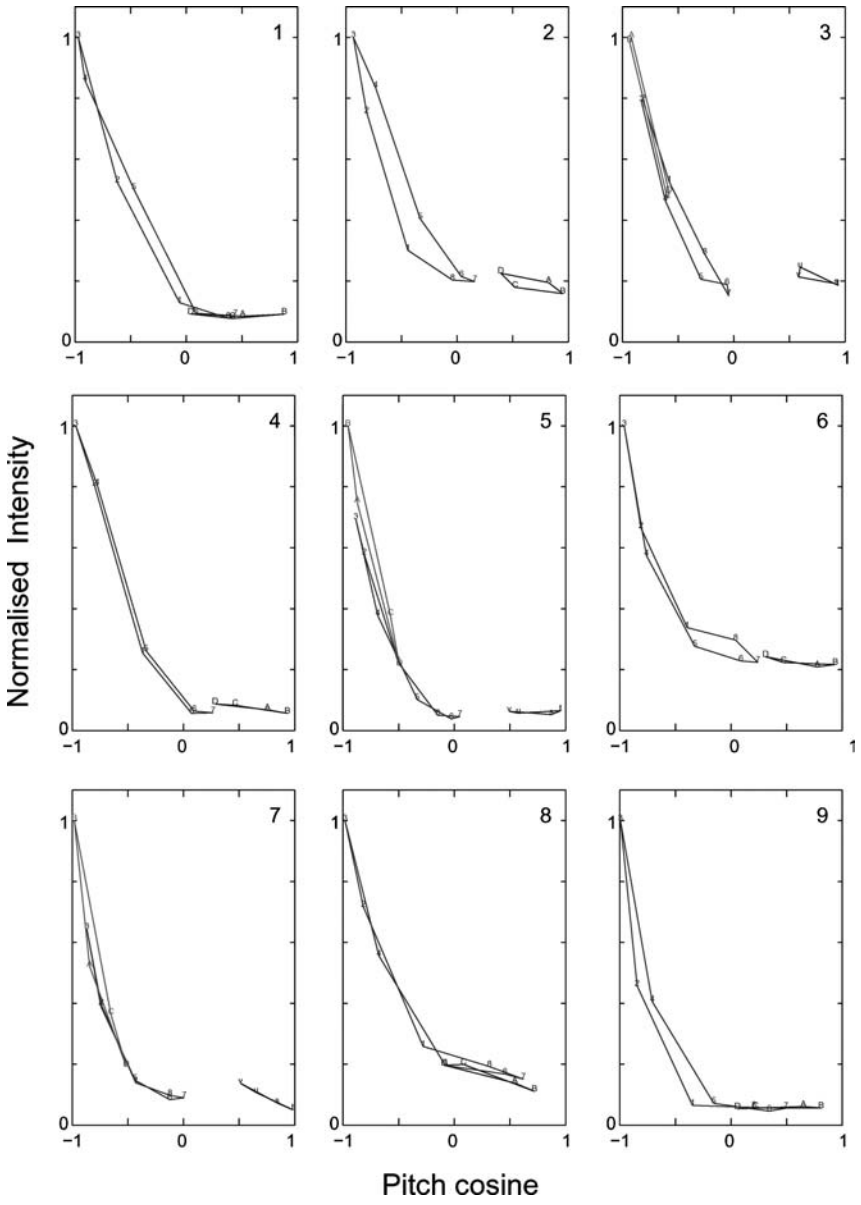

Figure 7. The electron pitch-angle distributions for the peak intensity of the nine events (see text). The electron energy channels are DE2 (53–103 keV, green), E′2 (64–112 keV, red) and E2 (60–107 keV, blue). The event number is indicated at the *top right* of each plot.

prior to 20:00 UT the radio corona was quiet. The first type III event was seen starting at or below 14 MHz at 21:00 UT on 26 June. This was the only type III event in the 24 h we are studying to start above 10 MHz, as seen above the background level. We have tentatively indicated with numbers in the upper and

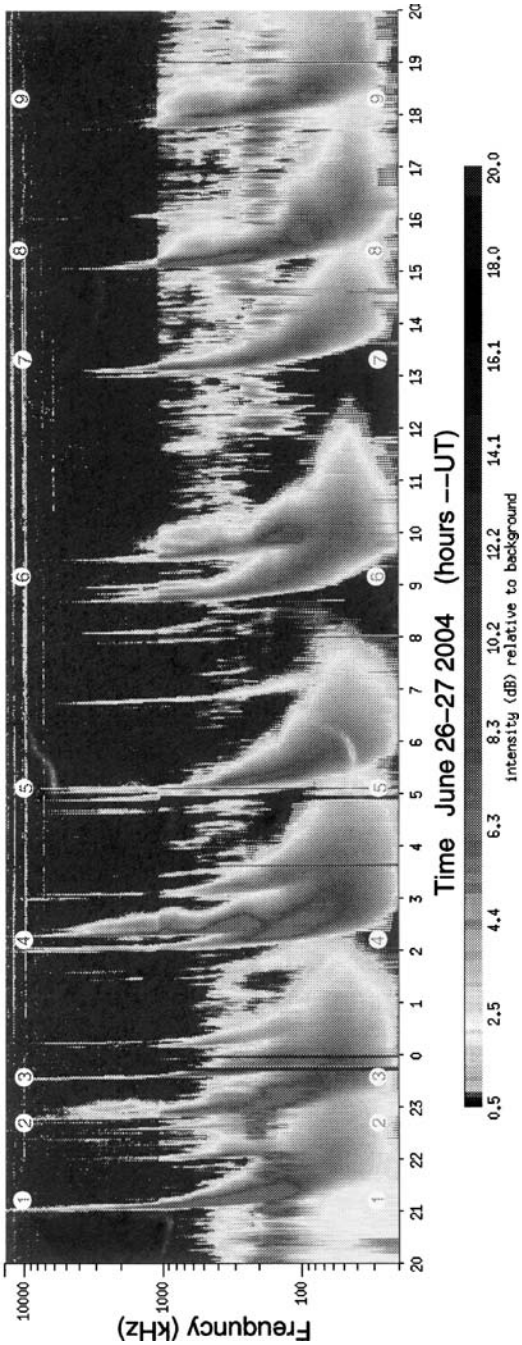

Figure 8. The RAD2 and RAD1 dynamic radio spectrum for 26 June 20:00 UT–27 June 20:00 UT, 2004. (Data courtesy of Dr M.L. Kaiser) *Blue* indicates low intensity and *red* high intensity; the frequency range is from 20 kHz to 14 MHz. As an aid for the eye the event numbers are indicated at the *top* and *bottom* of the plot.

lower part of Figure 8 which radio events are associated with which bursts. One fact is immediately apparent from Figure 8, namely that the starting frequency of the bursts has a downward trend, albeit not monotonic, to the extent that burst 9 is barely visible in RAD2. This is seen most readily if one takes the frequency where the intensity registers as red. This is strongly suggestive of an acceleration process which is occurring progressively higher in the corona, with the final burst starting at a plasma frequency appropriate to a coronal location above $\sim 4 R_{\odot}$ (Leblanc, Dulk, and Bougeret, 1998)

If we examine the bursts at a frequency, say around 500 kHz, then every one of the nine identified bursts is present at an intensity level high enough to come into the purple colour scale. We note also that the two additional bursts seen in DE1 (see Section 2.1) have a radio signature; these result in a pair of radio events for bursts 4 and 6, which merge by the time they have reached a plasma frequency around 50 kHz. This is true of bursts 2 and 3, which are probably a similar pair. Note that the criterion for defining a burst was that it should appear as a resolved intensity spike in both DE1 and DE2. Note also that there are a few fainter events which do not show up very prominently in the lower frequencies of RAD1, and do not contribute to a resolved electron event, although they may contribute to the electron intensity at an unresolvable level. Alternatively they may be electron events where the spectrum does not extend out to the lower threshold of DE1.

2.3. Other solar observations

As pointed out in Section 2.1, the Sun was particularly quiet during the 24 h of interest here. We have examined the SOHO/LASCO coronagraph data for this period. The corona was quiet on 26 and 27 June. In seeking associations of coronagraph images with the electron events, we restrict ourselves to events seen in projection on the western side of the Sun. We now give some details of events seen by LASCO in the 24-h period of interest. The first event is at a position angle of around 285°, which has a speed of around 300 km/s with a projected onset (nominally extrapolated back to $1 R_{\odot}$) around 20:30 UT. At the time of the onset of the first event this would have been at around $2 R_{\odot}$, and thus there is a plausible temporal and spatial association of this event with the LASCO CME. The position angle is conventionally measured anticlockwise from the solar north pole.

The next event is a very slow, gradually accelerating event which had a probable onset between events 5 and 6 and is not associated with either. The only other plausible CME-associations are with event 7 (a small, faint jet, with a speed of around 770 km/s, which becomes invisible by $\sim 6 R_{\odot}$) and event 8 (also a small, faint jet similar to the first one).

To summarise the LASCO observations, the only *classical* CME association was with event 1. We regard a *classical* CME as one with a width of 40° or more, with clear structure, and which can be seen in LASCO out to $10 R_{\odot}$ or more.

There was no optical Hα flare reported in *Solar Geophysical Data* for this period; however there was no flare patrol from 26 June 20:00 to 23:28 UT. There was only one flare above the GOES X-ray class C1 and this was a C2.3 flare with a maximum at 15:57 UT. This was not in time coincidence near any of the electron events, allowing up to 30 min propagation delay. There was only one short period of activity reported at any of the fixed radio frequencies covered in *Solar Geophysical Data*, and these were two short bursts at 245 MHz (of 5 and 7 min duration) between 09:17 and 09:58 UT. The closest burst to these times was burst 6 at ~08:42 UT. There was also faint emission reported from 09:00 to 11:00 UT at 127 MHz. There were very few metric type III radio bursts reported by *Solar Geophysical Data*. The only ones in time association with the decametric bursts were for events 4 and 5. Surprisingly, there was not one for event 1, which suggests that the starting altitude for this event may indeed have been around $2R_{\odot}$.

Thus this period is extremely quiet regarding emission associated with low coronal or chromospheric activity.

3. Discussion

The short impulsive electron beams which were emitted from the Sun over a 24-h period did not have any noteworthy chromospheric emission associated with them. There was not a single report of any microwave activity (*Solar Geophysical Data*) and the Sun was extremely quiet for a whole solar rotation (11 June to 8 July). Thus we can safely say that these electron beams were not flare-associated even allowing for particle trapping. Low level X-ray activity was in time coincidence with events 4–7, but below GOES X-ray class C1, and we regard this level as not very significant in terms of energetic electron acceleration. The LASCO coronagraphs also observed very little activity which might have been associated with the electron beams.

The electron events were all strongly field-aligned (Figure 7) and short-lived, typically lasting around 30 min in DE1 at full width 1/3 maximum. The relative constancy of the four sectors plotted in Figure 1 indicates that the propagation conditions in the interplanetary medium were remarkably stable. For example, in DE1 throughout this period, Sector 2 is highest, then Sector 1, then Sector 3, and finally Sector 4. This trend is maintained even in the periods between the bursts, with few exceptions.

The peak intensity, even in event 5, is about two orders of magnitude less than the intensity of the largest flare-associated events seen by ACE/EPAM over the lifetime since launch in 1997. Thus the events we are discussing, although large in the solar rotation covered, are relatively insignificant in the long-term history of solar electron events. The energy spectrum of the events is steep, and although we have represented it as a power law in energy, this is for convenience and consistency. We have no evidence that the spectrum for any of the events does not cut off close

to the lower energy end of the highest channel observed. Nevertheless, this does not invalidate our finding that the energy spectra are steep, consistent with the spectra reported by Potter, Lin, and Anderson (1980) for coronal events at lower energy.

We now turn to our explanation for these events. The similarity of the intensity time profiles and the energy spectrum suggest that the physical process(es) responsible is (are) the same for all events. First, they are not from flares. Second, they are not from CMEs. Third, the lack of metric radio emission rules out an origin in the low corona/chromosphere. We are then left with a coronal origin as the most likely explanation. As to the mechanism, one would suppose that a strong candidate for the energy source would be magnetic reconnection, such as proposed by Petschek (1964). Such a mechanism would predict outward moving jets from the reconnection site, which are consistent with the LASCO observations of events 7 and 8. However, the provenance of weak LASCO events is difficult to establish conclusively, and the visibility of jets from Petschek reconnection would be strongly dependent on the viewing angle with respect to the geometry of the reconnecting magnetic fields.

We have noted a slight tendency for the spectral index to be more negative as the series of events progresses, and also that the starting altitude of the decametric type III radio burst also has a slight tendency to increase with event number. This is consistent with an acceleration process that is a function of any or all of: magnetic field strength, ambient density, or inverse scale size. All these typically decrease as the coronal altitude increases.

Previous observations of coronal electrons (Potter, Lin, and Anderson, 1980; Lin, 1985) have concentrated on the smaller events, especially those where the spectrum could be observed down to 2 keV. Reames, Von Rosenvinge, and Lin (1985) emphasised that these events were often accompanied by ^{3}He-rich events, and that they had a significantly different spectral shape to the big flare events. Furthermore, Kahler, Reames, and Sheeley (2001) have shown that there is an association of jet-like CMEs with ^{3}He-rich events. We have shown above that some of the events discussed are accompanied by faint CME jets, and there is evidence (D. V. Reames, private communication, 2005) that there is some ^{3}He enhancement on June 27.

The events we are discussing therefore indicate that the coronal acceleration process is capable of accelerating not only events with a peak intensity up to $\sim$1% of the largest flare events, but up to an energy of at least around 200 keV. Although we have fitted a power law to the measured spectrum (see Figure 5) this is for consistency purposes only so that we have some basis for comparing the different events. We have no evidence that the spectrum continues as a power law to energies above around 200 keV, so that from our study, this may be taken as the highest proven energy.

The period we are discussing was at an unusually quiet time for all forms of solar activity. Therefore for the purpose of interpreting the decametric radio data, we will make the assumption that the corona was stable and could be represented by the

density model assumed by Leblanc, Dulk, and Bougeret (1998). Event 1 was not detected at metric wavelengths, but it was detected by WAVES/RAD2 on WIND at 14 MHz. The decametric type III bursts associated with events 2–4 appeared to start around 9–10 MHz, following which there was a decline in starting frequency to around 5–3 MHz, while event 9 was only detected below ∼1.1 MHz. Therefore, under the assumption made above, the radio data indicate that the electron beams were produced at an altitude starting with event 1 around $2R_\odot$, and generally increasing in altitude through the high corona ($\sim 4R_\odot$ for events 6–8) until the last event, 9, at an even higher altitude.

Some of the events are *double* events, in that a second, smaller event occurs within an hour of the first event, before it has decayed back to the local background intensity. We offer no explanation for this behaviour.

Examination of Figure 8 shows several faint type III bursts which we have not specifically identified. We have not been able to identify any associated electron event in DE1. This suggests that the acceleration process is going on at levels below that which produces a detectable near-relativistic electron event, but it does produce electrons sufficient to generate type III emission. This was noted by Potter, Lin, and Anderson (1980) whose events typically did not extend above 15 keV.

In summary, either the coronal accelerator is capable of accelerating much more intense and energetic electrons than previously thought, or there are strong shocks driven by erupting magnetic fields, which do not involve enough excess mass to be visible to coronagraphs. As there is no specific reason to invoke the latter, Occam's razor would favour the former.

4. Conclusions

We pointed out in the Introduction that there are at least three separate sources of near-relativistic (i.e., above 100 keV) solar electrons. These are flare-associated electrons which may often have hard spectra in the 30–300 keV region ($\gamma < 3$). Then there are electrons accelerated by CME-driven shocks (Simnett, Roelof, and Haggerty, 2002), which by their very nature are often mixed with flare electrons, which makes determination of their characteristic spectrum more difficult. Finally there are the coronal electrons, which have been known for many years to exist at low energies, but from this study we now know they may extend to energies up to or above 200 keV.

We argue that the quiet solar conditions eliminate flare-produced electrons, as there were virtually no flares. The same argument probably applies to CME-driven shocks, as apart from events 1, 7 and 8 there were no CMEs. The coronal events associated with events 7 and 8 were small jets, just visible in LASCO. Thus we can eliminate a large shock fronts. We need to be careful, however, in dismissing CMEs completely, as a CME is only visible in LASCO if the erupting structure contains significant excess mass. However, it is not the excess mass that accelerates

the electrons, and it is plausible that an erupting magnetic structure could drive a shock, while containing little excess mass over the ambient corona. With this caveat, we therefore conclude that the electrons we are studying here are accelerated in the high corona by a process that is not related to either flares or CMEs.

Thus the "coronal accelerator" is capable of accelerating much more intense and energetic electrons than previously thought, and therefore must be considered potentially as a major source of electrons both to propagate into the interplanetary medium and to be used as a seed population for CME-driven shocks and the solar flare accelerator.

Acknowledgements

The author wishes to thank his colleagues on the ACE and *Ulysses* teams for their help in making the data available and in a useable form. Dr M. L. Kaiser kindly supplied Figure 8 and Dr D. V. Reames provided helpful comments on the manuscript. Starlink computing facilities were used for the detailed analysis.

References

Bougeret, J.-L., *et al.*: 1995, *Space Sci. Rev.* **71**, 231.
Brueckner, G. E., *et al.*: 1995, *Solar Phys.* **162**, 357.
Gold, R. E., *et al.*: 1998, *Space Sci. Rev.* **86**, 541.
Kahler, S. W., Reames, D. V., and Sheeley, N. R., Jr.: 2001, *Astrophys. J.* **562**, 558.
Leblanc, Y., Dulk, G. A., and Bougeret, J.-L.: 1998, *Solar Phys.* **183**, 165.
Lin, R. P.: 1985, *Solar Phys.* **100**, 537.
Petschek, H.: 1964, in W. N. Hess (ed.), *Physics of Solar Flares*, NASA SP-50, 425.
Potter, D. W., Lin, R. P., and Anderson, K. A.: 1980, *Astrophys. J.* **235**, L97.
Reames, D. V.: 1999, *Space Sci. Rev.* **90**, 413.
Reames, D. V., Von Rosenvinge, T. T., and Lin, R. P.: 1985, *Astrophys. J.* **292**, 176.
Simnett, G. M., Roelof, E. C., and Haggerty, D. K.: 2002, *Astrophys. J.* **579**, 854.